Biological Psychiatry: CNNI

Novel Machine Learning Identifies Brain Patterns Distinguishing Diagnostic Membership of Human Immunodeficiency Virus, Alcoholism, and Their Comorbidity of Individuals

Ehsan Adeli, Natalie M. Zahr, Adolf Pfefferbaum, Edith V. Sullivan, and Kilian M. Pohl

ABSTRACT

The incidence of alcohol use disorder (AUD) in human immunodeficiency virus (HIV) infection is twice that of the rest of the population. This study documents complex radiologically identified, neuroanatomical effects of AUD+HIV comorbidity by identifying structural brain systems that predicted diagnosis on an individual basis. Applying novel machine learning analysis to 549 participants (199 control subjects, 222 with AUD, 68 with HIV, 60 with AUD+HIV), 298 magnetic resonance imaging brain measurements were automatically reduced to small subsets per group. Significance of each diagnostic pattern was inferred from its accuracy in predicting diagnosis and performance on six cognitive measures. While all three diagnostic patterns predicted the learning and memory score, the AUD+HIV pattern was the largest and had the highest predication accuracy (78.1%). Providing a roadmap for analyzing large, multimodal datasets, the machine learning analysis revealed imaging phenotypes that predicted diagnostic membership of magnetic resonance imaging scans of individuals with AUD, HIV, and their comorbidity.

Keywords: Alcoholism, Brain imaging, Comorbidity, Disease patterns, HIV infection, Machine learning

https://doi.org/10.1016/j.bpsc.2019.02.003

Alcohol use disorder (AUD) is common (1), and its comorbidity in individuals with human immunodeficiency virus (HIV) infection is high (2–4), occurring at a rate twice that of the general population (5). AUD and HIV infection each disrupts brain structural integrity with the likely outcome of reducing health-related quality of life and cognition (3,4). AUD targets, among other regions, the frontal cortices (6–8) and cerebellum (9,10). HIV similarly compromises the frontal cortices, but also the cingulate and parietal regions [e.g., (11)]. AUD and HIV are independently associated with volume deficits in the thalamus, hippocampus, caudate, and putamen [e.g., AUD (4,10,12), HIV (4,11,13)]. Relatively few brain studies have examined the heightened burden of disease comorbidity (2,14), which has the potential to exacerbate the untoward effects on neural systems through synergistic or additive processes (15,16). AUD+HIV shows moderate to severe abnormalities, especially in frontal cortices and thalamus (17).

One possible solution to enhance understanding of the complex neurological effects of AUD+HIV comorbidity is to encode the architecture of the whole brain of an individual through large numbers of measures extracted from a fine-grained parcellation of brain regions. To date, however, morphometric brain studies on AUD and HIV have relied on univariate testing of relatively few magnetic resonance imaging (MRI) metrics that are separately related to diagnostic groups (2,3,11,14–16,18–21). Alternatively, machine learning approaches (22–25) can jointly analyze a large number of metrics by combining them into a single score. To highlight the power of such multivariate analysis (22,26) for expanding knowledge about neuropsychiatric disorders, we derived diagnostic scores to predict diagnosis from MRIs collected in individuals with AUD, HIV, or their comorbidity.

To test the hypothesis that MRIs can be used to predict diagnosis and cognitive measures in individuals with AUD, HIV, or their comorbidity, we first improved on a technology called sparse classification (27–29). We then applied the corresponding novel machine learning analysis to a dataset of 549 MRIs of control subjects and individuals diagnosed with one of the three disorders, taken from our previous report on 30 regional volumes (17). Each MRI was now quantified in terms of 298 brain regional metrics of volume, surface area, thickness, and curvature. For each disorder, our data-driven approach first identified a diagnostic pattern by automatically reducing the large number of MRI metrics to a small subset affected by the disorder. The subset of metrics was then applied to each individual MRI to compute a diagnostic score to predict diagnosis and cognitive ramifications in the corresponding participant. By doing so, our machine learning analysis identified structural differences from control subjects in individuals not only with AUD [as in Guggenmos *et al.* (30)], but also with HIV and AUD+HIV comorbidity.

SEE COMMENTARY ON PAGE 508

ISSN: 2451-9022

METHODS AND MATERIALS

Participants

The four groups comprised 199 healthy control subjects (CTRL), 222 individuals with AUD (AUD), 68 HIV-infected individuals (HIV), and 60 subjects with AUD and HIV infection (AUD+HIV). Participants ranged in age between 25 and 75 years.

Participants with AUD were screened to meet DSM-IV criteria for alcohol dependence or abuse and DSM-5 criteria for AUD, have ≥10 years of heavy drinking, and habitually consume ≥150 drinks a month for men or ≥90 for women. The study recorded their days after last drink, total lifetime alcohol consumed in kilograms, and alcohol consumed in the past year.

Participants in the non-AUD groups (e.g., the HIV and CTRL groups) met neither DSM-IV criteria for alcohol dependence or abuse nor DSM-5 criteria for AUD. HIV group subjects were seropositive for the HIV infection with CD4 count >100 cells/μL (average: 303.0) and had a Karnofsky score ≥70 (31). Participants in the CTRL group had never met DSM-IV or DSM-5 criteria for any neuropsychiatric disorder and tested negative for HIV infection. The two HIV groups had higher mean Veterans Aging Cohort Study indices (32) than either the CTRL or AUD groups (Table 1). Note that the Veterans Aging Cohort Study defines a score based on preassigned points for age, HIV indicators (CD4 count and HIV-1 RNA), and general indicators of organ system injury (see Supplement for details).

Participants completed neuropsychological tests assessing six cognitive, motor, and social functional domains. Composite scores of each domain were derived from age- and education-corrected *Z* scores based on control performance: verbal language, executive function, learning and memory (LM), speed of information processing, motor skills, and quality of social functioning. Table 1 lists their mean ± SD as well as the medication history of participants (see Supplement for details).

The neuropsychological scores were based on the means of composite scores representing six functional domains [cf. (33,34)] described previously [Supplemental Material in Pfefferbaum *et al*. (17)]. Raw scores from tests included in each composite score were age-corrected, based on 66 male and 85 female healthy control subjects who were 20 to 67 years of age at their first examination, and expressed as standardized *Z* scores. All metrics (e.g., speed scores such as Trails A and B) were transformed so that higher scores were in the direction of better performance. Each of the composite scores was the mean of the *Z* scores of available test measures for each participant: executive function comprised Trail Making Test Part B (35) or Color Trails 2 (36) time, Wechsler Memory Scale–Revised (37) or MicroCog (38) forward and backward digit span, and the Stroop Color and Word Test raw score (39); LM comprised the Rey–Osterrieth Complex Figure Test immediate recall raw score (40) and Wechsler Memory Scale–Revised Logical Memory index (immediate recall total raw score) (37) or MicroCog Memory index (immediate recognition score) (38); verbal language comprised FAS letter fluency total score (41) and National Adult Reading Test (42), Peabody (43), or Wechsler Test of Adult Reading (44) total score; speed of information processing comprised Trail Making Test Part A (35) or Color Trails 1 (36) time, digit symbol (45) or symbol digit (46) raw score, and Stroop Color and Word Test raw score (40); motor skills comprised the grooved pegboard test mean of left and right hand scores (47), fine finger movement test mean of all conditions (48), and ataxia mean score of standing on the left and right legs separately (49); and quality of social functioning comprised 21-Item Short Form Survey Quality of Life total raw score (50), Global Assessment of Functioning score (current) (51), and activities of daily living (combined performance and instrumental scores) (52). Participants underwent different cognitive tests for some domains because some tests were replaced during the longitudinal study.

MRI Data Acquisition and Preprocessing

Imaging data were acquired on a 3T SIGNA system (GE Healthcare, Waukesha, WI) using an eight-channel Array Spatial Sensitivity Encoding Technique coil for parallel and accelerated imaging. Inversion recovery–spoiled gradient recalled echo sequence (repetition time = 7.068 ms, inversion time = 300 ms, echo time = 2.208 ms, flip angle = 15°, 256 × 256 matrix, slice dimensions = 1.25 mm × 0.9375 mm × 0.9375 mm, 124 slices) were collected in the sagittal plane.

Processing of a T1-weighted MR image (see Supplement for details) resulted in the supratentorial volume according to the SRI24 atlas (53) and the *Z* scores of 298 morphometric measurements extracted by FreeSurfer (54–56). Note that baseline volumetric MRI data of the 549 participants were previously published (17) but were derived solely from 30 regions of interest (ROIs) of the SRI24 atlas (53), rather than the FreeSurfer atlas used herein.

The morphometric measurements of the CTRL group varied significantly with age, sex, and supratentorial volume (Pearson correlation $p < .005$). These confounding factors were regressed out from the morphometric measurements by parameterizing a general linear model (57) on the control subjects of the training data. Details can be found in Supplement.

Machine Learning for Statistical Analysis

The data were divided into three diagnosis-specific sets: AUD ($n = 222$) versus CTRL ($n = 199$) groups, HIV ($n = 68$) versus CTRL ($n = 199$) groups, and AUD+HIV ($n = 60$) versus CTRL ($n = 199$) groups. With respect to each dataset, our analysis followed the three steps outlined in Figure 1. Specifically, we first identified a diagnostic pattern by applying a multivariate machine learning method [see Adeli *et al.* (27)] (see Supplement for details) to the entire dataset (step 1), which also automatically matched the sample size of the two cohorts. The resulting pattern was applied to individual MRIs producing a diagnostic score, which was the prediction of an individual's having the diagnosis based solely on brain MRI measurements. The perfect diagnostic score for CTRL group was 0.0; for any individual from the diagnostic group, the perfect diagnostic score was 1.0. The diagnostic pattern was also correlated with the six cognitive scores recorded for members of that diagnostic group (step 2). Correlations that were positive and had a p value <.05 were reported. Step 3 measured the accuracy of the machine learning method via 10-fold

Table 1. Demographic Information and the Statistics of the Cognitive and Clinical Measures for Each Group

	CTRL Group (n = 199)	AUD Group (n = 222)	p Value (vs. CTRL Group)	HIV Group (n = 68)	p Value (vs. CTRL Group)	AUD+HIV Group (n = 60)	p Value (vs. CTRL Group)	Pairwise Group Differences[a]
Demographic Variables								
Female/male	92 (46)/107 (54)	66 (30)/156 (70)	4.8108×10^{-4}	21 (31)/47 (69)	.0017	22 (37)/38 (63)	<.00001	$\chi^2_1 = 13.4$, $p = .004$
Age, years	46.7 ± 14.2	48.4 ± 9.9	NS	51.4 ± 8.7	.0102	51.7 ± 6.9	.0118	CTRL = AUD < HIV = AUD+HIV
Education, years	16.0 ± 2.3	13.4 ± 2.4	<.00001	13.5 ± 2.4	<.00001	13.0 ± 2.1	<.00001	CTRL > AUD = HIV = AUD+HIV
Socioeconomic status (lower value means higher status)	25.5 ± 11.6	40.9 ± 14.4	<.00001	40.7 ± 14.2	<.00001	45.2 ± 12.2	<.00001	CTRL < AUD = HIV = AUD+HIV
Body mass index, kg/m^2	25.9 ± 4.2	26.8 ± 4.8	.0408	26.6 ± 4.7	NS	26.8 ± 4.9	NS	CTRL = AUD = HIV = AUD+HIV
Asian/African American/Caucasian/other	28/28/127/16	4/71/117/30	<.00001	0/31/34/3	<.00001	0/38/17/5	<.00001	$\chi^2_1 = 97.80$, $p < .0001$
Clinical Variables								
Days after last drink	–	196.9 ± 507.9	–	–	–	398.9 ± 1126.8	–	AUD = AUD+HIV
Total lifetime alcohol consumed, kg	34.0 ± 57.0	1206.2 ± 885.7	7.4523×10^{-40}	110.5 ± 240.7	NS	1081.0 ± 916.1	4.9219×10^{-28}	CTRL = HIV < AUD = AUD+HIV
Alcohol consumed in past year, kg	–	42.2 ± 45.7	–	–	–	14.0 ± 17.7	–	AUD > AUD+HIV
VACS index	13.8 ± 12.3	15.0 ± 12.7	NS	27.3 ± 18.1	4.6496×10^{-7}	32.8 ± 22.5	5.1148×10^{-9}	CTRL = AUD < HIV = AUD+HIV
CD4 cell count (100/mm^3)	–	–	–	303.0 ± 188.7	–	278.9 ± 216.5	–	HIV = AUD+HIV
Nadir CD4 (100/mm^3)	–	–	–	202.0 ± 176.4	–	208.5 ± 174.4	–	HIV = AUD+HIV
Viral load	–	–	–	2.13 ± 1.14	–	2.24 ± 1.18	–	HIV = AUD+HIV
On HAART medication, %	–	–	–	88	–	87	–	HIV = AUD+HIV ($\chi^2_1 = 0.0457$)
With AIDS status, %	–	–	–	53	–	60	–	HIV = AUD+HIV ($\chi^2_1 = 0.9968$)
Cognitive Variables								
Verbal language	−0.10 ± 0.86	−0.70 ± 0.96	2.0424×10^{-5}	−0.92 ± 1.14	3.7039×10^{-6}	−0.71 ± 0.99	2.5637×10^{-4}	CTRL > AUD = HIV = AUD+HIV
Executive function	−0.04 ± 0.90	−0.70 ± 1.12	3.7239×10^{-6}	−0.98 ± 1.55	4.7593×10^{-6}	−1.12 ± 1.43	9.3434×10^{-8}	CTRL > AUD = HIV = AUD+HIV
Learning and memory	−0.08 ± 0.80	−0.95 ± 0.86	8.5698×10^{-11}	−0.84 ± 0.97	2.8087×10^{-6}	−1.08 ± 0.88	7.0479×10^{-10}	CTRL > AUD = HIV = AUD+HIV
Speed of information processing	0.14 ± 0.69	−0.39 ± 0.90	5.8493×10^{-6}	−0.51 ± 0.85	8.5445×10^{-7}	−0.82 ± 1.01	4.6449×10^{-10}	CTRL > AUD = HIV = AUD+HIV
Motor skills, ms	−0.10 ± 0.77	−0.72 ± 0.90	4.1689×10^{-7}	−0.93 ± 1.36	5.6897×10^{-6}	−0.96 ± 1.44	1.0281×10^{-5}	CTRL > AUD = HIV = AUD+HIV
Quality of social functioning	0.15 ± 0.75	−2.00 ± 1.63	2.2572×10^{-38}	−1.94 ± 1.47	1.6003×10^{-30}	−2.80 ± 1.96	4.8170×10^{-36}	CTRL > AUD = HIV = AUD+HIV

Values are n (%) or mean ± SD unless otherwise indicated. Each of the composite scores was the mean of available test measures for each participant (refer to the text for details). Group differences are measured for each diagnosis group with respect to the CTRL group by χ^2 test (for sex, ethnicity, HAART medication, and AIDS status) and t test (for other measures), and are considered NS if $p > .05$.

AIDS, acquired immunodeficiency syndrome; AUD, alcohol use disorder; CTRL, control; HAART, highly active antiretroviral therapy; HIV, human immunodeficiency virus; NS, not significant; VAC, Veterans Aging Cohort Study.

[a]An equals sign (=) indicates that groups were not significantly different; and less than (<) and greater than (>) symbols indicate that groups were significantly different ($p < .05$).

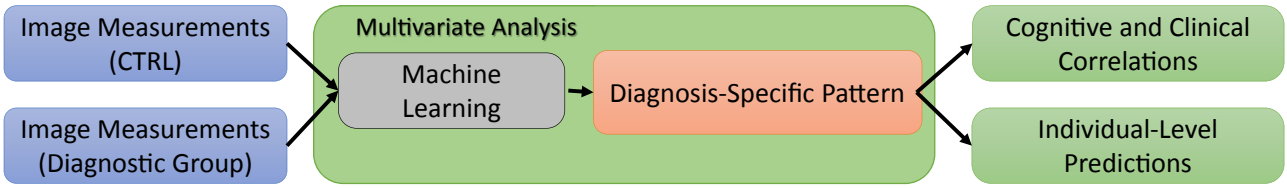

Figure 1. The analysis approach used for identifying diagnostic pattern and score specific to alcohol use disorder, human immunodeficiency virus, and alcohol use disorder and human immunodeficiency virus comorbidity. It includes three major steps: multivariate analysis for identification of diagnostic pattern and score (step 1), cognitive correlations (step 2), and individual-level predictions (step 3). CTRL, control group.

cross-validation (58). The balanced accuracy (27), specificity, and sensitivity in predicting the diagnosis of each test subject were recorded. Furthermore, the significance of the accuracy ($p < .001$) was inferred using the Fisher exact test (59). A detailed description of the three steps appears in the Supplement.

RESULTS

Multivariate Analysis: Diagnostic Patterns

The diagnostic patterns are listed in Table 2 and visualized in Figure 2 (omitting white matter hypointensities). The AUD-specific pattern consisted of measures from 13 unique brain ROIs, the HIV-specific pattern of 15 brain ROIs, and the AUD+HIV–specific pattern of 25 brain ROIs. All patterns included the surface area of the posterior cingulate and the volumes of the white matter hypointensities, precentral gyrus, thalamus, and hippocampus. Seven additional measures from the AUD+HIV pattern overlapped with either the AUD or the HIV pattern and included the mean curvature of the banks of the superior temporal sulcus and the average thickness of the superior frontal and superior parietal gyri.

Cognitive Correlations

Table 3 summarizes the correlations among the diagnostic patterns and the six cognitive measures. All three diagnostic patterns significantly predicted lower LM scores. Furthermore, executive function was significantly correlated with the AUD pattern, whereas speed of information processing was significantly correlated with the HIV and AUD+HIV patterns. As shown in Figure 3, these performance scores had lower values with higher diagnostic scores, i.e., greater certainty of an individual to be diagnosed with the condition. Testing the diagnostic pattern of AUD with lifetime alcohol consumption and that of HIV with Veterans Aging Cohort Study and CD4 measures did not reveal significant correlations.

Table 2. Measures Associated With Each Diagnostic Pattern

Group	Volume	Surface Area	Mean Curvature	Average Thickness
AUD	Superior frontal[a] Precentral gyrus[a] Thalamus[a] Caudate Hippocampus[a] Accumbens WM hypointensities[a]	Posterior cingulate[a]	Bankssts[a] Lingual Insula	Lateral orbitofrontal Pars triangularis Postcentral Insula
HIV	Parahippocampal Posterior cingulate Precentral gyrus[a] Superior parietal Thalamus[a] Hippocampus[a] Accumbens WM hypointensities[a]	Supramarginal[a] Inferior temporal[a] Temporal pole[a] Pericalcarine[a] Posterior cingulate[a] Insula	Precuneus Posterior cingulate Insula	Superior frontal[a] Superior parietal[a] Inferior temporal Middle temporal Insula
AUD+HIV	Superior frontal[a] Frontal pole Pars opercularis Pars triangularis Precentral gyrus[a] Precuneus Thalamus[a] Caudate Putamen Hippocampus[a] WM hypointensities[a]	Superior frontal Caudal middle frontal Paracentral Medial orbitofrontal Supramarginal[a] Bankssts Entorhinal Inferior temporal[a] Temporal pole[a] Lateral occipital Pericalcarine[a] Posterior cingulate[a] Rostral anterior cingulate	Medial orbitofrontal Paracentral Pars orbitalis Bankssts[a] Entorhinal Parahippocampal Pericalcarine	Superior frontal[a] Frontal pole Medial orbitofrontal Superior parietal[a]

AUD, alcohol use disorder; Bankssts, banks of the superior temporal sulcus; HIV, human immunodeficiency virus; WM, white matter.
[a]Measure in the AUD or HIV pattern that was also in the AUD+HIV pattern.

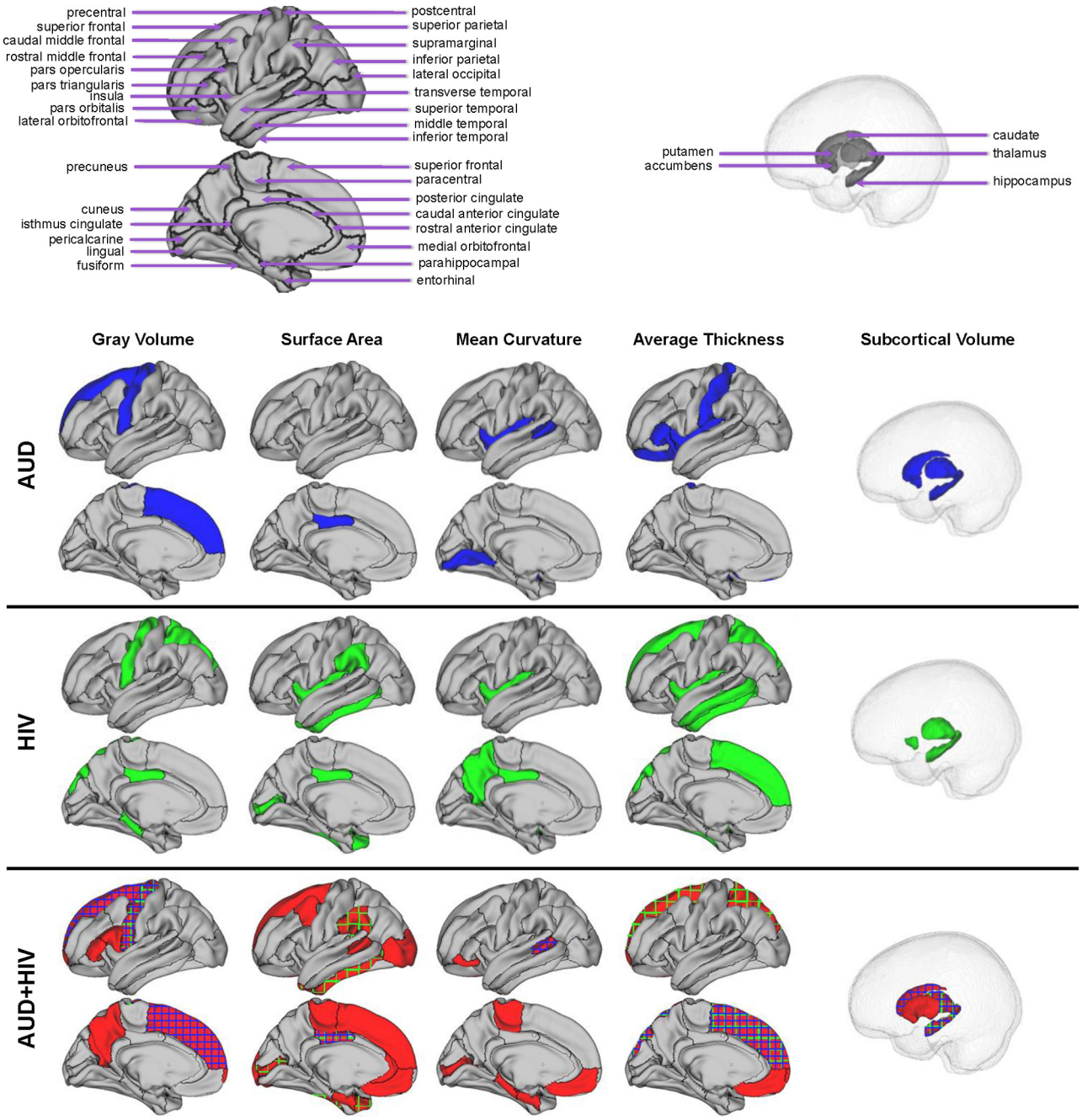

Figure 2. The diagnostic patterns (see also Table 2) for alcohol use disorder (AUD), human immunodeficiency virus (HIV) infection, and AUD+HIV comorbidity. Measures in the HIV (purple) or AUD (green) pattern also appearing in the comorbidity pattern are shown in plaid in AUD+HIV.

Individual-Level Prediction

All three diagnostic scores predicted the diagnosis of individuals with significantly high accuracies. The balanced accuracy of the diagnostic score for the AUD versus CTRL group was 70.1%, for the HIV versus CTRL group was 76.2%, and for the AUD+HIV versus CTRL group was 78.1%. The ranking of the three accuracy scores agreed with the size of the diagnostic pattern, i.e., the AUD group pattern was the smallest (with 15 regional measurements), followed by the HIV (22 measurements) and AUD+HIV (35 measurements) groups (Table 2). As each pattern inferred its own diagnostic score, each subject of the control group had a diagnostic score specific to each diagnosis. As expected, diagnostic scores of the CTRL group subjects were generally lower than those of disease-affected participants (Figure 4).

Table 3. Correlation Between the Pattern Identified for Each Diagnosis Group and the Six Cognitive Scores

Group	Verbal Language	Executive Function	Learning and Memory	Speed of Information Processing	Motor Skills	Quality of Social Functioning
AUD		✓	✓			
HIV			✓	✓		
AUD+HIV			✓	✓		

Check mark (✓) indicates significant correlation ($p < .05$). Cognitive scores were measured through tests outlined in the Supplement.
AUD, alcohol use disorder; HIV, human immunodeficiency virus.

DISCUSSION

The outcome of this machine learning analysis supported the hypothesis that MRIs alone can predict diagnosis and cognitive scores of AUD, HIV, or AUD+HIV. Our approach reduced the 298 brain measures to those most informing diagnosis, i.e., the diagnostic pattern, and then applied the pattern to the MRIs of individuals to compute each person's diagnostic score. Doing so preserved the statistical power of the data because testing for significance did not require multiple comparison correction, as is the case for conventional univariate analysis. Conventional studies minimize the number of comparisons by preselecting measurements [e.g., gray matter volume (11) or average thickness (60)] or creating summary scores (17) deemed informative according to expert domain knowledge. Scores then rely on univariate testing that entails a group-level analysis to correlate each score with each

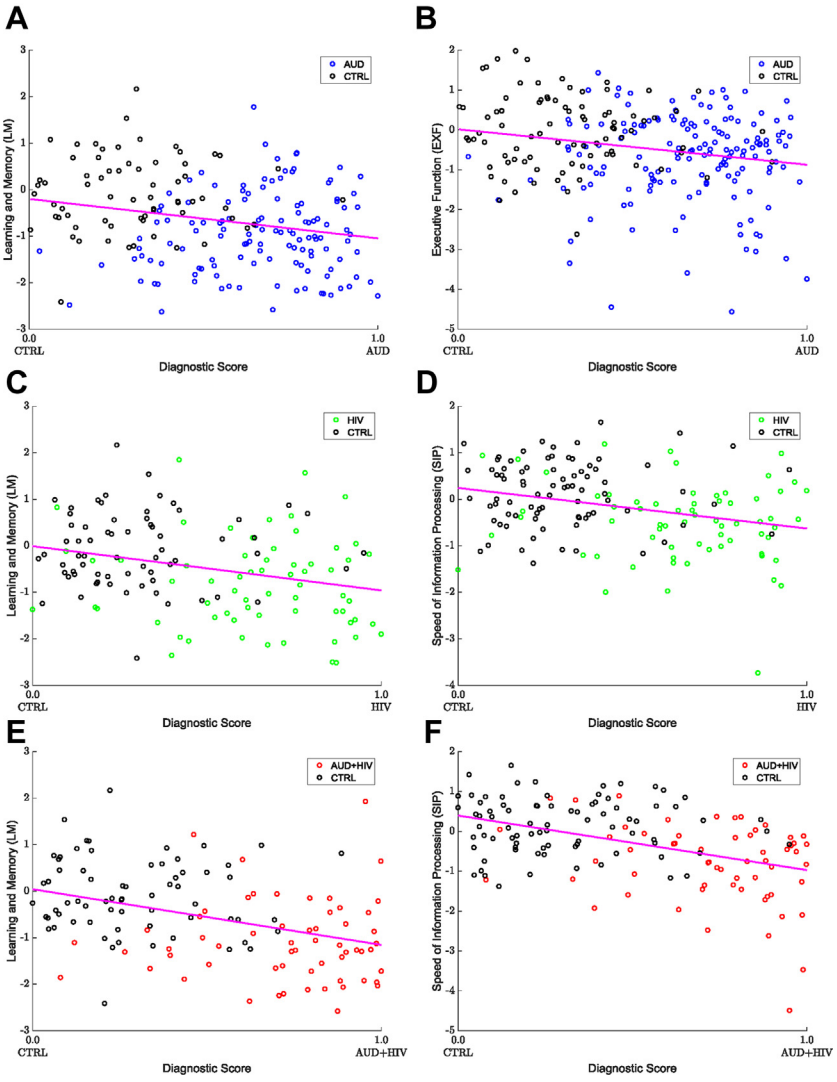

Figure 3. Cognitive measures significantly correlating with the diagnostic scores. The cognitive scores decrease as diagnostic scores increase. **(A)** The learning and memory (LM) measure as a function of diagnostic score, for the alcohol use disorder (AUD) vs. control (CTRL) group; **(B)** the executive function (EXF) measure as a function of diagnostic score, for the AUD vs. CTRL group; **(C)** the LM measure as a function of diagnostic score, for the human immunodeficiency virus (HIV) vs. CTRL group; **(D)** the speed of information processing (SIP) measure as a function of diagnostic score, for the HIV vs. CTRL group; **(E)** the LM measure as a function of diagnostic score, for the AUD+HIV vs. CTRL group; and **(F)** the SIP measure as a function of diagnostic score, for the AUD+HIV vs. CTRL group.

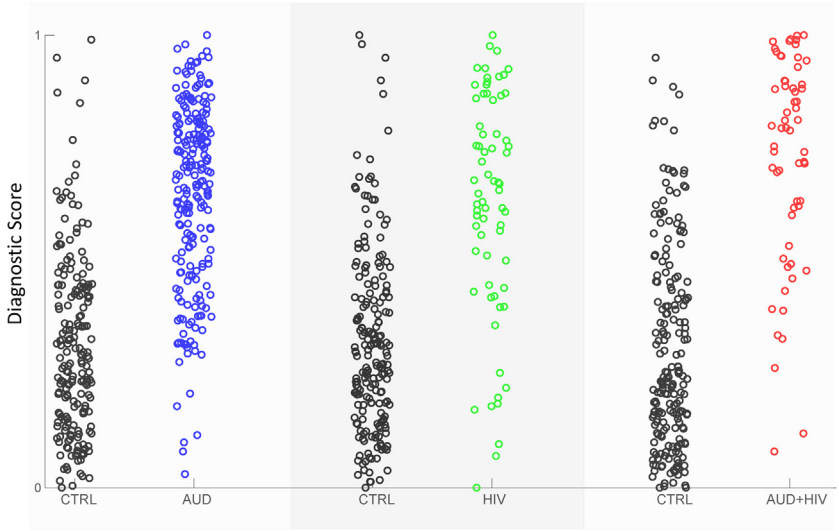

Figure 4. Diagnostic scores for each sample with respect to the three diagnosis-specific group comparisons (control [CTRL] group vs. alcohol use disorder [AUD] group, CTRL group vs. human immunodeficiency virus [HIV] group, CTRL group vs. AUD+HIV group).

diagnosis. A powerful alternative to this conventional analysis is the proposed machine learning technology, which, as noted in the Supplement, was also more accurate in predicting diagnosis than other multivariate approaches. Not only did the novel machine learning approach predict AUD or HIV diagnosis of individuals based solely on their MRIs, but the predictive power of the identified patterns was measured on unseen data (i.e., data not used for optimizing the approach) so that the patterns could serve as imaging phenotypes in other MRI studies of AUD or HIV.

We recognize that this article presents a secondary analysis of data previously published in Pfefferbaum *et al.* (17). Unlike the original study, we omitted hepatitis C coinfection from the analysis, but our analysis was still confined by the much smaller number of HIV-infected patients (HIV and AUD+HIV) than the CTRL cohort and the AUD group. For our analysis to be impartial to this issue, the machine learning method automatically selected an equal number of samples from each group and trained its model on this balanced dataset. Furthermore, we measured the prediction power using the balanced accuracy metric, which accounted for unequal sample sizes. The scores indicated that our approach produced accurate findings even in case of imbalanced data.

Human MRI studies of HIV or AUD have used machine learning analysis to predict the age of participants (61,62) or to select MRI metrics related to a diagnosis (63–67). A hallmark of the proposed analysis was the diagnostic score of individuals (see Figure 4), which was a continuous score directly linking variation in MRI metrics to diagnosis. This link enabled a refined interpretation of significant correlations between diagnostic patterns and functional ramifications of the condition. For example, all three diagnostic patterns predicted the LM score (see Table 3) and consisted of regions closely linked to this brain function, namely, the hippocampus (68–70), thalamus (71,72), and posterior cingulate cortex (73,74). The hippocampus and thalamus have been identified as targets of AUD (75) and HIV (13,76,77), and AUD+HIV comorbidity has been shown to principally affect the thalamus (4,78). Cingulate volume is more frequently reported as compromised in the HIV literature relative to the AUD literature [e.g., (78–82)]. While the imaging literature has typically reported on gray matter volume effects, studies that assess cortical thickness rather than cortical volume can show different results. For example, HIV has been shown to compromise cortical thickness of areas such as the insula and temporal cortices (83–85).

Also reported for all three conditions was the link between lower LM scores and higher diagnostic scores (Figure 3). According to our machine learning model, a higher diagnostic score reflected a greater impact of the disorder on the regional measures defining the diagnostic pattern. Thus, the diagnostic scores and patterns accurately summarized the magnitude of the impact that each disorder had on an affected metric.

An interesting observation was the inclusion of the hippocampus in the patterns of all groups. As it is reported in the literature (13,86), this region supports learning and memory. Based on the statistics reported in Table 1, this cognitive measure was also significantly impaired across all three groups compared with the CTRL cohort.

Critically, our findings support a compounding effect of AUD and HIV on the neural systems of individuals diagnosed with both conditions. Among the three conditions, the diagnostic pattern of the comorbidity was the largest consisting of 35 regional measures. Several of these measures featured as part of the AUD and HIV pattern and were selected by the AUD+HIV pattern, with the exception of the mean curvature and average thickness of the insula (see Table 2); however, neither the mean curvature nor the average thickness measure was selected by all three patterns. Rather, the patterns of the three diagnoses converged on volumes of four regions (precentral gyrus, hippocampus, thalamus, white matter hypointensities) and one surface area (posterior cingulate cortex). Consistent with the size of the diagnostic patterns was the prediction accuracy of the diagnostic scores, which was most accurate for AUD+HIV comorbidity (78.1% balanced

accuracy). While the accuracy scores might be further improved based on the discussion in the Supplement, all these findings indicate that the combined impact of AUD and HIV on the brain system was more extensive than either condition alone.

In addition to overlap among the three diagnostic patterns, the comorbidity pattern contained elements specific to each single diagnosis. The HIV and AUD+HIV patterns were highly accurate in predicting speed of information processing performance, which is known to decline faster in patients with HIV (87,88) and AUD (89) than in the healthy individuals. Speed of information processing has been also linked to regions that were part of both patterns, notably, the superior frontal cortex (90,91), precentral gyrus (92), superior parietal lobe (93,94), inferior temporal lobe (90,95,96), pericalcarine gyrus (90), supramarginal gyrus (97,98), and temporal pole (99). Featured in both patterns was the thalamus, whose volume has been reported to be significantly smaller in the HIV population, with (4,80) or without (4,11,13) AUD comorbidity. Appearing in both the AUD and the comorbidity pattern was the volume of the superior frontal cortex (17,100), which has been observed to be smaller in AUD than in control subjects (18,101). The significant correlation between executive function and the diagnostic pattern was reported with respect to the AUD group, but not for the comorbidity cohort. This inconsistency might be explained by executive functioning's being negatively affected by alcohol consumption, which was more recent and prevalent in the AUD cohort. Their number of days after last drink was significantly shorter ($p = .0012$; two-sided t test), and their amount of alcohol consumed in past year was significantly greater ($p < .001$; two-sided t test) than were those in the AUD+HIV cohort. Interestingly, these findings further supported the compounding effect of AUD and HIV, as their combined effects lead to a higher prediction accuracy than the AUD-specific pattern extracted on a cohort with higher alcohol consumption.

Note that we only reported on the compounding effect, as the machine learning analysis could not quantitatively assess the additive or interactive characteristic of an effect. Furthermore, the subject-level inference from this type of analysis often does not accord with the results of group-level analysis (102). For instance, quality of social functioning was the cognitive score most strongly differentiating between control subjects and the three cohorts. However, the score neither significantly correlated with any of the diagnostic patterns nor distinguished individuals. In this dataset, a better predictor for identifying significant correlations was the variance of a score within a diagnostic group. For each diagnostic group, the corresponding diagnostic patterns significantly correlated with the cognitive scores' having the smallest variation, which was speed of information processing for the HIV cohort and LM for the other two diagnoses. This observation is in line with the analysis performed in step 2 of Figure 1, as the corresponding correlation was sensitive toward the within-class covariance.

Another limitation of this study was the assumption that samples were healthy or diagnosed with HIV, AUD, or their comorbidity. One could thus increase the significance of the data-driven predictions by measuring the prediction accuracies of the diagnostic scores on the MRIs of participants with other diagnoses. However, the prediction accuracy was determined on unseen data so that the findings of this study could apply to other MRI studies adhering to this assumption. Specifically, we measured the accuracy of our machine learning method using 10-fold cross-validation (step 3 in Figure 1). To avoid reporting overly optimistic findings, cross-validation parameterized the Z scores (with respect to the control subjects) and the proceeding method (including sample selection) on a subset of the data (training), and then the accuracy of the method was measured on the remaining data, which avoided reporting overly optimistic findings. One drawback of this process is that our method identified a unique diagnostic pattern for each training run. Discussing the common denominator of the 10 different patterns is complex and requires statistics over the entire dataset. To simplify, we focused the discussion for each diagnosis on an example of a diagnostic pattern, which was created by applying the machine learning approach on the entire diagnostic dataset (step 1 in Figure 1).

Finally, we caution against drawing conclusions about measurements omitted from diagnostic patterns presented here, as these measurements can also be informative with respect to a diagnosis. However, they were not picked by the machine learning approach, which identified a constellation of measurements that achieved a higher accuracy in labeling the individuals of the training data. Changing the training data (as done in cross-validation) can lead to selecting a different pattern. Thus, the diagnostic patterns presented in this article should be viewed as an example of a family of patterns that lead to similar prediction accuracy.

Conclusions

We report on the diagnostic patterns and scores based on MRI data that predicted diagnostic classification of individuals with AUD, HIV, or their comorbidity relative to control patterns. Novel machine learning technology automatically reduced 298 MRI brain measures to small subsets implicated by each diagnostic group, eliminating the need for expert-driven input. The impact of a disorder on the diagnostic pattern was summarized by a diagnostic score, which revealed an exacerbated effect of AUD+HIV comorbidity. The diagnostic patterns and scores also predicted cognitive performance of individuals and their accuracy was measured on unseen data. Thus, they could serve as imaging phenotypes for studies investigating AUD, HIV, and their comorbidity. The entire analysis was data driven so that the novel machine learning approach is readily applicable to MRI studies of other neuropsychiatric conditions and also enables repurposing of multimetric data.

ACKNOWLEDGMENTS AND DISCLOSURES

This work was supported by U.S. National Institute on Alcohol Abuse and Alcoholism Grant Nos. AA017347 (to NMZ, AP, EVS), AA005965 (to NMZ, AP), AA010723 (to EVS), AA017168 (to EVS), AA026762 (to EA), and MH113406 (to KMP); and the Moldow Women's Hope and Healing Fund (to EVS).

We thank Dr. Stephanie A. Sassoon for providing insight into the clinical testings.

The authors report no biomedical financial interests or potential conflicts of interest.

ARTICLE INFORMATION

From the Department of Psychiatry and Behavioral Sciences (EA, NMZ, AP, EDV, KMP), Stanford School of Medicine, Stanford; and the Center for Biomedical Sciences (NMZ, AP, KMP), SRI International, Menlo Park, California.

Address correspondence to Kilian M. Pohl, Ph.D., Program Director of Biomedical Computing, SRI International, 333 Ravenswood Avenue, Menlo Park, CA 94025; E-mail: kilian.pohl@stanford.edu.

Received Oct 5, 2018; revised and accepted Feb 15, 2019.

Supplementary material cited in this article is available online at https://doi.org/10.1016/j.bpsc.2019.02.003.

REFERENCES

1. Management of Substance Abuse Unit of the World Health Organization (2014): Global Status Report on Alcohol and Health, 2014. Geneva, Switzerland: World Health Organization.
2. Gongvatana A, Morgan EE, Iudicello JE, Letendre SL, Grant I, Woods SP, *et al.* (2014): A history of alcohol dependence augments HIV-associated neurocognitive deficits in persons aged 60 and older. J Neurovirol 20:505–513.
3. Fama R, Sullivan EV, Sassoon SA, Pfefferbaum A, Zahr NM (2016): Impairments in component processes of executive function and episodic memory in alcoholism, HIV infection, and HIV infection with alcoholism comorbidity. Alcohol Clin Exp Res 40:2656–2666.
4. Pfefferbaum A, Rosenbloom MJ, Sassoon SA, Kemper CA, Deresinski S, Rohlfing T, *et al.* (2012): Regional brain structural dysmorphology in human immunodeficiency virus infection: Effects of acquired immune deficiency syndrome, alcoholism, and age. Biol Psychiatry 72:361–370.
5. Justice A, Sullivan L, Fiellin D, Veterans Aging Cohort Study Project T (2010): HIV/AIDS, comorbidity, and alcohol: Can we make a difference? Alcohol Res Health 33:258–266.
6. Cardenas VA, Studholme C, Meyerhoff DJ, Song E, Weiner MW (2005): Chronic active heavy drinking and family history of problem drinking modulate regional brain tissue volumes. Psychiatry Res 138:115–130.
7. Pfefferbaum A, Sullivan EV, Mathalon DH, Lim KO (1997): Frontal lobe volume loss observed with magnetic resonance imaging in older chronic alcoholics. Alcohol Clin Exp Res 21:521–529.
8. Cardenas VA, Studholme C, Gazdzinski S, Durazzo TC, Meyerhoff DJ (2007): Deformation-based morphometry of brain changes in alcohol dependence and abstinence. Neuroimage 34:879–887.
9. Sullivan EV, Rose J, Pfefferbaum A (2006): Effect of vision, touch and stance on cerebellar vermian-related sway and tremor: A quantitative physiological and MRI study. Cereb Cortex 16:1077–1086.
10. Sullivan EV, Pfefferbaum A (2009): Neuroimaging of the Wernicke-Korsakoff syndrome. Alcohol Alcohol 44:155–165.
11. Pfefferbaum A, Rogosa DA, Rosenbloom MJ, Chu W, Sassoon SA, Kemper CA, *et al.* (2014): Accelerated aging of selective brain structures in human immunodeficiency virus infection: A controlled, longitudinal magnetic resonance imaging study. Neurobiol Aging 35:1755–1768.
12. Le Berre AP, Pitel AL, Chanraud S, Beaunieux H, Eustache F, Martinot JL, *et al.* (2014): Chronic alcohol consumption and its effect on nodes of frontocerebellar and limbic circuitry: Comparison of effects in France and the United States. Hum Brain Mapp 35:4635–4653.
13. Wade BS, Valcour V, Busovaca E, Esmaeili-Firidouni P, Joshi SH, Wang Y, *et al.* (2015): Subcortical shape and volume abnormalities in an elderly HIV+ cohort. Proc SPIE Int Soc Opt Eng 9417:9417S.
14. Fama R, Rosenbloom MJ, Nichols BN, Pfefferbaum A, Sullivan EV (2009): Working and episodic memory in HIV infection, alcoholism, and their comorbidity: Baseline and 1-year follow-up examinations. Alcohol Clin Exp Res 33:1815–1824.
15. Bernardin F, Maheut-Bosser A, Paille F (2014): Cognitive impairments in alcohol-dependent subjects. Front Psychiatry 5:78.
16. Heaton RK, Franklin DR, Ellis RJ, McCutchan JA, Letendre SL, Leblanc S, *et al.* (2011): HIV-associated neurocognitive disorders before and during the era of combination antiretroviral therapy: Differences in rates, nature, and predictors. J Neurovirol 17:3–16.
17. Pfefferbaum A, Zahr NM, Sassoon SA, Kwon D, Pohl KM, Sullivan EV (2018): Accelerated and premature aging characterizing regional cortical volume loss in human immunodeficiency virus infection: Contributions from alcohol, substance use, and hepatitis C coinfection. Biol Psychiatry Cogn Neurosci Neuroimaging 3:844–859.
18. Manzo G, De Gennaro A, Cozzolino A, Serino A, Fenza G, Manto A (2014): MR imaging findings in alcoholic and nonalcoholic acute Wernicke's encephalopathy: A review. Biomed Res Int 2014:503596.
19. Avants BB, Epstein CL, Grossman M, Gee JC (2008): Symmetric diffeomorphic image registration with cross-correlation: Evaluating automated labeling of elderly and neurodegenerative brain. Med Image Anal 12:26–41.
20. Crovitz HF, Zener K (1962): A group-test for assessing hand- and eye-dominance. Am J Psychol 75:271–276.
21. Rosenbloom MJ, Sullivan EV, Sassoon SA, O'Reilly A, Fama R, Kemper CA, *et al.* (2007): Alcoholism, HIV infection, and their comorbidity: Factors affecting self-rated health-related quality of life. J Stud Alcohol Drugs 68:115–125.
22. Bzdok D (2017): Classical statistics and statistical learning in imaging neuroscience. Front Neurosci 11:543.
23. Smith SM, Nichols TE (2018): Statistical challenges in "big data" human neuroimaging. Neuron 97:263–268.
24. Varoquaux G, Thirion B (2014): How machine learning is shaping cognitive neuroimaging. Gigascience 3:28.
25. Castiglioni I, Salvatore C, Ramirez J, Gorriz JM (2018): Machine-learning neuroimaging challenge for automated diagnosis of mild cognitive impairment: Lessons learnt. J Neurosci Methods 302:10–13.
26. Zhang Y, Kwon D, Esmaeili-Firidouni P, Pfefferbaum A, Sullivan EV, Javitz H, *et al.* (2016): Extracting patterns of morphometry distinguishing HIV associated neurodegeneration from mild cognitive impairment via group cardinality constrained classification. Hum Brain Mapp 37:4523–4538.
27. Adeli E, Li X, Kwon D, Zhang Y, Pohl KM (2019): Logistic regression confined by cardinality-constrained sample and feature selection [published online ahead of print Feb 26]. IEEE Trans Pattern Anal Mach Intell.
28. Adeli E, Shi F, An L, Wee CY, Wu G, Wang T, *et al.* (2016): Joint feature-sample selection and robust diagnosis of Parkinson's disease from MRI data. Neuroimage 141:206–219.
29. Hastie T, Tibshirani R, Wainwright M (2015): Statistical Learning With Sparsity: The Lasso and Generalizations. Boca Raton, FL: CRC Press.
30. Guggenmos M, Scheel M, Sekutowicz M, Garbusow M, Sebold M, Sommer C, *et al.* (2018): Decoding diagnosis and lifetime consumption in alcohol dependence from grey-matter pattern information. Acta Psychiatr Scand 137:252–262.
31. Karnofsky DA, Burchenal JH (1949): The clinical evaluation of chemotherapeutic agents in cancer. In: MacLeod CM, editor. Evaluation of Chemotherapeutic Agents: New York, Columbia University Press, 196.
32. Justice AC, Dombrowski E, Conigliaro J, Fultz SL, Gibson D, Madenwald T, *et al.* (2006): Veterans Aging Cohort Study (VACS): Overview and description. Med Care 44:S13–S24.
33. Antinori A, Arendt G, Becker JT, Brew BJ, Byrd DA, Cherner M, *et al.* (2007): Updated research nosology for HIV-associated neurocognitive disorders. Neurology 69:1789–1799.
34. Sacktor N, Skolasky RL, Seaberg E, Munro C, Becker JT, Martin E, *et al.* (2016): Prevalence of HIV-associated neurocognitive disorders in the Multicenter AIDS Cohort Study. Neurology 86:334–340.
35. Tombaugh TN (2004): Trail Making Test A and B: Normative data stratified by age and education. Arch Clin Neuropsychol 19:203–214.

36. D'Elia L, Satz P (1989): Color Trails 1 and 2. Odessa, FL: Psychological Assessment Resources.
37. Bowden SC, Bell RC (1992): Relative usefulness of the WMS and WMS-R: A comment on D'Elia et al. (1989). J Clin Exp Neuropsychol 14:340–346.
38. Elwood RW (2001): MicroCog: Assessment of cognitive functioning. Neuropsychol Rev 11:89–100.
39. Golden C (1978): Stroop Color and Word Test: A Manual for Clinical and Experimental Uses. Chicago: Stoelling Co.
40. Bennett-Levy J (1984): Determinants of performance on the Rey-Osterrieth complex figure test: An analysis, and a new technique for single-case assessment. Br J Clin Psychol 23:109–119.
41. Borkowski JG, Benton AL, Spreen O (1967): Word fluency and brain damage. Neuropsychologia 5:135–140.
42. Nelson HE (1982): The National Adult Reading Test (NART). Windsor, Canada: Nelson.
43. Dunn LM, Dunn ES (1997): Peabody Picture Vocabulary Test, 3rd ed. Circle Pines, MN: American Guidance Service.
44. Wechsler D (2001): Wechsler Test of Adult Reading. San Antonio, TX: Pearson Education, Inc.
45. Hart R, Kwentus J, Wade J, Hamer R (1987): Digit symbol performance in mild dementia and depression. J Consult Clin Psychol 55:236–238.
46. Smith A (1973): The Symbol Digit Modalities Test Manual. Los Angeles: Western Psychological Services.
47. Trites RL (1977): The Grooved Pegboard Test. Neuropsychological Test Manual. Ottawa, Canada: Royal Ottawa Hospital.
48. Fama R, Eisen JC, Rosenbloom MJ, Sassoon SA, Kemper CA, Deresinski S, *et al.* (2007): Upper and lower limb motor impairments in alcoholism, HIV infection, and their comorbidity. Alcohol Clin Exp Res 31:1038–1044.
49. Fregly AR (1968): An ataxia battery not requiring rails. Aerosp Med 39:277–282.
50. Bozzette SA, Hays RD, Berry SH, Kanouse DE, Wu AW (1995): Derivation and properties of a brief health status assessment instrument for use in HIV disease. J Acquir Immune Defic Syndr Hum Retrovirol 8:253–265.
51. Moos RH, McCoy L, Moos BS (2000): Global assessment of functioning (GAF) ratings: Determinants and role as predictors of one-year treatment outcomes. J Clin Psychol 56:449–461.
52. Katz S (1983): Assessing self-maintenance activities of daily living, mobility and instrumental activities of daily living. J Am Geriatr Soc 31:721–727.
53. Rohlfing T, Zahr NM, Sullivan EV, Pfefferbaum A (2010): The SRI24 multichannel atlas of normal adult human brain structure. Hum Brain Mapp 31:798–819.
54. Dale AM, Fischl B, Sereno MI (1999): Cortical surface-based analysis. I. Segmentation and surface reconstruction. Neuroimage 9:179–194.
55. Reuter M, Schmansky NJ, Rosas HD, Fischl B (2012): Within-subject template estimation for unbiased longitudinal image analysis. Neuroimage 61:1402–1418.
56. Fischl B (2012). FreeSurfer. Neuroimage 62:774–781.
57. Madsen H, Thyregod P (2010): Introduction to General and Generalized Linear Models. Boca Raton, FL: CRC Press.
58. Arlot S, Celisse A (2010): A survey of cross-validation procedures for model selection. Stat Surv 4:39.
59. Fisher RA (1935): The logic of inductive inference. J R Stat Soc 98:39–82.
60. Thompson PM, Dutton RA, Hayashi KM, Toga AW, Lopez OL, Aizenstein HJ, *et al.* (2005): Thinning of the cerebral cortex visualized in HIV/AIDS reflects CD4 + T lymphocyte decline. Proc Natl Acad Sci U S A 102:15647–15652.
61. Kuhn T, Kaufmann T, Doan NT, Westlye LT, Jones J, Nunez RA, *et al.* (2018): An augmented aging process in brain white matter in HIV. Hum Brain Mapp 39:2532–2540.
62. Cole JH, Underwood J, Caan MW, De Francesco D, van Zoest RA, Leech R, *et al.* (2017): Increased brain-predicted aging in treated HIV disease. Neurology 88:1349–1357.
63. Squeglia LM, Ball TM, Jacobus J, Brumback T, McKenna BS, Nguyen-Louie TT, *et al.* (2017): Neural predictors of initiating alcohol use during adolescence. Am J Psychiatry 174:172–185.
64. Cao B, Kong X, Kettering C, Yu P, Ragin A (2015): Determinants of HIV-induced brain changes in three different periods of the early clinical course: A data mining analysis. Neuroimage Clin 9:75–82.
65. Wade BS, Valcour VG, Wendelken-Riegelhaupt L, Esmaeili-Firidouni P, Joshi SH, Gutman BA, *et al.* (2015): Mapping abnormal subcortical brain morphometry in an elderly HIV+ cohort. Neuroimage Clin 9:564–573.
66. Underwood J, Cole JH, Caan M, De Francesco D, Leech R, van Zoest RA, *et al.* (2017): Gray and white matter abnormalities in treated human immunodeficiency virus disease and their relationship to cognitive function. Clin Infect Dis 65:422–432.
67. Zhu X, Du X, Kerich M, Lohoff FW, Momenan R (2018): Random forest based classification of alcohol dependence patients and healthy controls using resting state MRI. Neurosci Lett 676:27–33.
68. Deng W, Aimone JB, Gage FH (2010): New neurons and new memories: How does adult hippocampal neurogenesis affect learning and memory? Nat Rev Neurosci 11:339–350.
69. Petersen RC, Jack CR Jr, Xu YC, Waring SC, O'Brien PC, Smith GE, *et al.* (2000): Memory and MRI-based hippocampal volumes in aging and AD. Neurology 54:581–587.
70. Bird CM, Burgess N (2008): The hippocampus and memory: Insights from spatial processing. Nat Rev Neurosci 9:182–194.
71. Aggleton JP, O'Mara SM, Vann SD, Wright NF, Tsanov M, Erichsen JT (2010): Hippocampal-anterior thalamic pathways for memory: Uncovering a network of direct and indirect actions. Eur J Neurosci 31:2292–2307.
72. de Bourbon-Teles J, Bentley P, Koshino S, Shah K, Dutta A, Malhotra P, *et al.* (2014): Thalamic control of human attention driven by memory and learning. Curr Biol 24:993–999.
73. Pearson JM, Heilbronner SR, Barack DL, Hayden BY, Platt ML (2011): Posterior cingulate cortex: Adapting behavior to a changing world. Trends Cogn Sci 15:143–151.
74. Leech R, Sharp DJ (2014): The role of the posterior cingulate cortex in cognition and disease. Brain 137:12–32.
75. Sullivan EV, Marsh L (2003): Hippocampal volume deficits in alcoholic Korsakoff's syndrome. Neurology 61:1716–1719.
76. Scott-Sheldon LA, Walstrom P, Carey KB, Johnson BT, Carey MP, Team MR (2013): Alcohol use and sexual risk behaviors among individuals infected with HIV: A systematic review and meta-analysis 2012 to early 2013. Curr HIV/AIDS Rep 10:314–323.
77. Sanford R, Fernandez Cruz AL, Scott SC, Mayo NE, Fellows LK, Ances BM, *et al.* (2017): Regionally specific brain volumetric and cortical thickness changes in HIV-infected patients in the HAART era. J Acquir Immune Defic Syndr 74:563–570.
78. Janssen MA, Meulenbroek O, Steens SC, Goraj B, Bosch M, Koopmans PP, *et al.* (2015): Cognitive functioning, wellbeing and brain correlates in HIV-1 infected patients on long-term combination antiretroviral therapy. AIDS 29:2139–2148.
79. Clark US, Walker KA, Cohen RA, Devlin KN, Folkers AM, Pina MJ, *et al.* (2015): Facial emotion recognition impairments are associated with brain volume abnormalities in individuals with HIV. Neuropsychologia 70:263–271.
80. Fama R, Rosenbloom MJ, Sassoon SA, Rohlfing T, Pfefferbaum A, Sullivan EV (2014): Thalamic volume deficit contributes to procedural and explicit memory impairment in HIV infection with primary alcoholism comorbidity. Brain Imaging Behav 8:611–620.
81. Agudelo M, Khatavkar P, Yndart A, Yoo C, Rosenberg R, Devieux JG, *et al.* (2014): Alcohol abuse and HIV infection: Role of DRD2. Curr HIV Res 12:234–242.
82. Ances BM, Ortega M, Vaida F, Heaps J, Paul R (2012): Independent effects of HIV, aging, and HAART on brain volumetric measures. J Acquir Immune Defic Syndr 59:469–477.

83. Kallianpur KJ, Kirk GR, Sailasuta N, Valcour V, Shiramizu B, Nakamoto BK, *et al.* (2012): Regional cortical thinning associated with detectable levels of HIV DNA. Cereb Cortex 22:2065–2075.
84. Sanford R, Fellows LK, Ances BM, Collins DL (2018): Association of brain structure changes and cognitive function with combination antiretroviral therapy in HIV-positive individuals. JAMA Neurol 75:72–79.
85. Adeli E, Kwon D, Zhao Q, Pfefferbaum A, Zahr NM, Sullivan EV, *et al.* (2018): Chained regularization for identifying brain patterns specific to HIV infection. Neuroimage 183:425–437.
86. Anderson EB, Grossrubatscher I, Frank L (2014): Dynamic hippocampal circuits support learning- and memory-guided behaviors. Cold Spring Harb Symp Quant Biol 79:51–58.
87. Fellows RP, Byrd DA, Morgello S (2014): Effects of information processing speed on learning, memory, and executive functioning in people living with HIV/AIDS. J Clin Exp Neuropsychol 36:806–817.
88. Anand P, Springer SA, Copenhaver MM, Altice FL (2010): Neurocognitive impairment and HIV risk factors: A reciprocal relationship. AIDS Behav 14:1213–1226.
89. Tzambazis K, Stough C (2000): Alcohol impairs speed of information processing and simple and choice reaction time and differentially impairs higher-order cognitive abilities. Alcohol Alcohol 35:197–201.
90. Dux PE, Tombu MN, Harrison S, Rogers BP, Tong F, Marois R (2009): Training improves multitasking performance by increasing the speed of information processing in human prefrontal cortex. Neuron 63:127–138.
91. Charlton RA, Landau S, Schiavone F, Barrick TR, Clark CA, Markus HS, *et al.* (2008): A structural equation modeling investigation of age-related variance in executive function and DTI measured white matter damage. Neurobiol Aging 29:1547–1555.
92. Carter CS, Mintun M, Cohen JD (1995): Interference and facilitation effects during selective attention: An H215O PET study of Stroop task performance. Neuroimage 2:264–272.
93. Gold BT, Powell DK, Xuan L, Jiang Y, Hardy PA (2007): Speed of lexical decision correlates with diffusion anisotropy in left parietal and frontal white matter: Evidence from diffusion tensor imaging. Neuropsychologia 45:2439–2446.
94. Nishiike S, Nakagawa S, Tonoike M, Takeda N, Kubo T (2001): Information processing of visually-induced apparent self motion in the cortex of humans: Analysis with magnetoencephalography. Acta Otolaryngol Suppl 545:113–115.
95. Ptak R, Valenza N (2005): The inferior temporal lobe mediates distracter-resistant visual search of patients with spatial neglect. J Cogn Neurosci 17:788–799.
96. Mruczek RE, Sheinberg DL (2007): Activity of inferior temporal cortical neurons predicts recognition choice behavior and recognition time during visual search. J Neurosci 27:2825–2836.
97. Perianez JA, Maestu F, Barcelo F, Fernandez A, Amo C, Ortiz Alonso T (2004): Spatiotemporal brain dynamics during preparatory set shifting: MEG evidence. Neuroimage 21:687–695.
98. Lazeron RH, Rombouts SA, Machielsen WC, Scheltens P, Witter MP, Uylings HB, *et al.* (2000): Visualizing brain activation during planning: The tower of London test adapted for functional MR imaging. AJNR Am J Neuroradiol 21:1407–1414.
99. Decety J, Cacioppo S (2012): The speed of morality: A high-density electrical neuroimaging study. J Neurophysiol 108:3068–3072.
100. Sullivan EV, Zahr NM, Sassoon SA, Thompson WK, Kwon D, Pohl KM, *et al.* (2018): The role of aging, drug dependence, and hepatitis C comorbidity in alcoholism cortical compromise. JAMA Psychiatry 75:474–483.
101. Zahr NM (2014): Structural and microstructral imaging of the brain in alcohol use disorders. Handb Clin Neurol 125:275–290.
102. Zhang Y, Kwon D, Pohl KM (2017): Computing group cardinality constraint solutions for logistic regression problems. Med Image Anal 35:58–69.